AIP | Applied Physics Letters

H-tailored surface conductivity in narrow band gap In(AsN)

A. V. Velichko, A. Patanè, M. Capizzi, I. C. Sandall, D. Giubertoni, O. Makarovsky, A. Polimeni, A. Krier, Q. Zhuang, and C. H. Tan

Citation: Applied Physics Letters **106**, 022111 (2015); doi: 10.1063/1.4906111
View online: http://dx.doi.org/10.1063/1.4906111
View Table of Contents: http://scitation.aip.org/content/aip/journal/apl/106/2?ver=pdfcov
Published by the AIP Publishing

H-tailored surface conductivity in narrow band gap In(AsN)

A. V. Velichko,[1,a)] A. Patanè,[1,a)] M. Capizzi,[2] I. C. Sandall,[3] D. Giubertoni,[4] O. Makarovsky,[1] A. Polimeni,[2] A. Krier,[5] Q. Zhuang,[5] and C. H. Tan[3]
[1]*School of Physics and Astronomy, The University of Nottingham, Nottingham NG7 2RD, United Kingdom*
[2]*Dipartimento di Fisica, Sapienza Università di Roma, Piazzale A. Moro 2, 00185 Roma, Italy*
[3]*Department of Electronic & Electrical Engineering, The University of Sheffield, Sheffield S1 3JD, United Kingdom*
[4]*Center for Materials and Microsystems—Fondazione Bruno Kessler, via Sommarive 18, 38123 Povo, Trento, Italy*
[5]*Physics Department, Lancaster University, Lancaster LA1 4YB, United Kingdom*

(Received 4 December 2014; accepted 6 January 2015; published online 14 January 2015)

We show that the *n*-type conductivity of the narrow band gap In(AsN) alloy can be increased within a thin (~100 nm) channel below the surface by the controlled incorporation of H-atoms. This channel has a large electron sheet density of $\sim 10^{18}\,m^{-2}$ and a high electron mobility ($\mu > 0.1$ $m^2V^{-1}s^{-1}$ at low and room temperature). For a fixed dose of impinging H-atoms, its width decreases with the increase in concentration of N-atoms that act as H-traps thus forming N-H donor complexes near the surface.
[http://dx.doi.org/10.1063/1.4906111]

The incorporation of low concentrations (~1%) of nitrogen-atoms in III-V semiconductor compounds acts to modify the electronic band structure of the host crystal, thus enabling band structure engineering and a fine tuning of fundamental electronic properties, such as the band gap energy.[1,2] An additional attractiveness of this class of compounds is the possibility of using post-growth hydrogenation, combined with electron beam lithography and masking[3] or laser writing,[4] to create distinct, tailor-made light emitting regions,[3,4] all integrated onto a single substrate. These effects rely on the ability of hydrogen to modulate the material optical properties by passivating the electronic activity of nitrogen through the formation of di-hydrogen N-H_2 complexes.[5]

Although the physics of hydrogen in wide-band gap dilute nitrides, such as Ga(AsN), has been researched both experimentally and theoretically, the effects of hydrogen on the electronic properties of narrow band gap III-N-Vs, such as In(AsN), are still largely unknown.[6–8] The mechanisms of hydrogen diffusion, H-N interaction, and, in particular, the passivation of the electronic activity of nitrogen by hydrogen, which is well established for wide bandgap III-N-Vs,[3] can be qualitatively different in narrow band gap compounds and may open perspectives in the exploitation of these materials in mid-infrared optoelectronics.[9] In particular, the narrow band gap InAs semiconductor has an electron accumulation layer in the surface region with a Fermi level, E_F, located well above the conduction band minimum.[10–12] Hydrogen, being either an unintentional or intentional dopant, can alter surface properties;[11] furthermore, the electronic behaviour of monoatomic-H can be modified by nitrogen through the formation of N-H donor complexes.[8]

In this Letter, we exploit the combined effects of nitrogen and hydrogen in InAs and show that the *n*-type conductivity of the In(AsN) alloy can be significantly increased within a thin (~100 nm) channel below the surface by the controlled incorporation of H-atoms. For a fixed dose of impinging H-atoms, the width of the surface conducting channel decreases with the increase in concentration of N-atoms, which act as H-traps, thus forming N-H donor complexes near the surface. The channel retains a high electron mobility ($\mu > 0.1$ $m^2V^{-1}s^{-1}$ at low and room temperature) with an electron sheet density of $10^{18}\,m^{-2}$, significantly larger than in N-free InAs. This controlled modification of the surface conductivity and large increase in the electron sheet density by hydrogen could provide a platform for several applications, such as gas and molecular sensing[12] and "all semiconductor" plasmonic waveguides.[13]

The nominally undoped In(AsN) epilayers (thickness $d = 1.0\,\mu m$ and N-content, [N], of 0, 0.15, 1.1, and 1.9%) were grown by Molecular Beam Epitaxy (MBE) on a semi-insulating (SI) (100)-oriented GaAs substrate, which provides effective isolation for electrical measurements. The wafers were spun with photoresist and patterned by standard photolithography into Hall bars. Metal contacts consisting of 40 nm of Ti followed by 400 nm of Au were deposited onto the samples to provide Ti-Au ohmic contacts. Hydrogen was implanted in the epilayers using a Kaufman source with ion current densities of a few tens of mA/m^2 and an ion-beam energy of 100 eV for a time t_H ranging from 9 min to 2 h, impinging H-doses $D_H = 10^{20}$ ions/m^2 ([N] > 0) and $D_H = 3 \times 10^{21}$ ions/m^2 ([N] = 0), at temperatures $T_H = 250$–$300\,^\circ C$. As shown later, these relatively low H-doses enable us to incorporate hydrogen near the surface of the In(AsN) epilayers.

To investigate the H-diffusion profile, the epilayer with [N] = 1.1% was irradiated with deuterium, ^2H, for which Secondary Ion Mass Spectrometry (SIMS) has a higher sensitivity. A Cs^+beam with energy of 1 keV incident at 55° on the sample surface was used in a CAMECA Sc-Ultra mass spectrometer and negative secondary ions ($^2H^-$, $^{75}As^-$,

[a)]Authors to whom correspondence should be addressed. Electronic addresses: amalia.patane@nottingham.ac.uk and anton.velychko@nottingham.ac.uk. Tel.:+44 115 9515185

$^{115}In^{-}$, and $^{75}As^{14}N^{-}$) were collected. For the magneto-transport studies, the magnetic field **B** was generated either by a superconducting magnet (up to 14 T) or a room temperature electromagnet (up to 1 T). The magnetic field was applied parallel to the growth axis z, *i.e.*, $\mathbf{B} = [0, 0, B]$, or at an angle θ relative to z.

Figure 1 shows the second derivative of the transverse magnetoresistance, d^2R_{xx}/d^2B, as a function of the inverse magnetic field, $1/B$, for both virgin (V) and hydrogenated (H) In(AsN) epilayers with [N] = 0.15% at $T = 2$ K. For the V-sample, we observe Shubnikov-de Haas (SdH) oscillations at $B > 1$ T with period $\Delta_L(1/B) = (0.26 \pm 0.02)\text{T}^{-1}$. Following the hydrogenation, an additional series of SdH oscillations emerge at $B > 3$ T with a shorter period $\Delta_S(1/B) = (0.012 \pm 0.001)\text{T}^{-1}$. These short-period oscillations are not observed in N-free InAs (see inset of Fig. 1) and persist for **B** tilted at various angles from $\theta = 0°$ to 90°. The positions in $1/B$ of the maxima/minima in d^2R_{xx}/d^2B do not scale as $1/B\cos\theta$, thus indicating that they are caused by the SdH effect in a 3D electron gas. The periods Δ_S and Δ_L give 3D electron densities of $n = (2e/\hbar\Delta)^{3/2}/(3\pi^2) = (4.2 \pm 0.5) \times 10^{24}\,\text{m}^{-3}$ and $(4.3 \pm 0.5) \times 10^{22}\,\text{m}^{-3}$, respectively.

All N-containing epilayers *hydrogenated under the same conditions* ($D_H = 10^{20}$ ions/m^2, $t_H \approx 9$ min, and $T_H = 250$–300 °C) exhibit a similar behavior, i.e., hydrogen induces an additional series of *short-period* SdH oscillations (see Figure 2(a)). With [N] increasing from 0.15 to 1.9%, these oscillations emerge at larger B, which corresponds to a decrease of the electron mobility, and the period Δ_S decreases from 0.012 to 0.0055 T^{-1}, which implies an increase in the electron density n_s from $4.2 \times 10^{24}\,\text{m}^{-3}$ to $1.4 \times 10^{25}\,\text{m}^{-3}$. These electron densities are almost two orders of magnitude higher than those found in the virgin samples and those derived from the *long-period* SdH oscillations, which vary from $n_b = 4.3 \times 10^{22}\,\text{m}^{-3}$ to $5.9 \times 10^{23}\,\text{m}^{-3}$, see Figure 2(b).

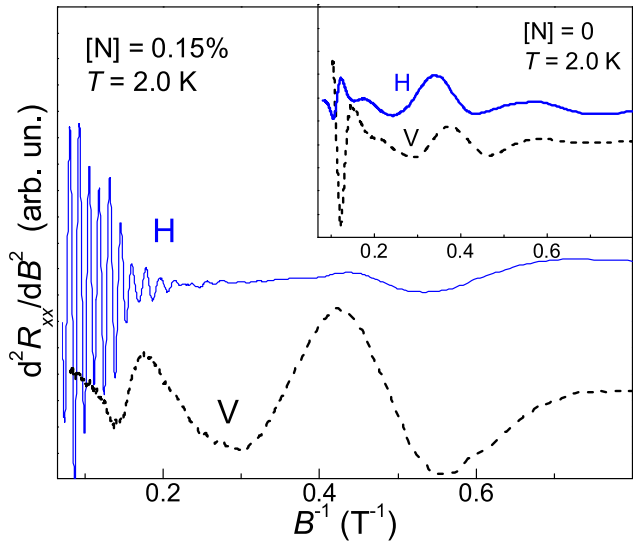

FIG. 1. Second derivative of the magnetoresistance, d^2R_{xx}/d^2B, as a function of the inverse magnetic field, $1/B$, at $T = 2$ K for a virgin (dashed line) and hydrogenated (solid line) In(AsN) epilayer with [N] = 0.15%. The hydrogenation conditions are $D_H = 10^{20}$ ions/m^2, $t_H = 9$ min, and $T_H = 300$ °C. Inset: d^2R_{xx}/d^2B versus $1/B$ for a virgin (dashed line) and hydrogenated (solid line) InAs epilayer.

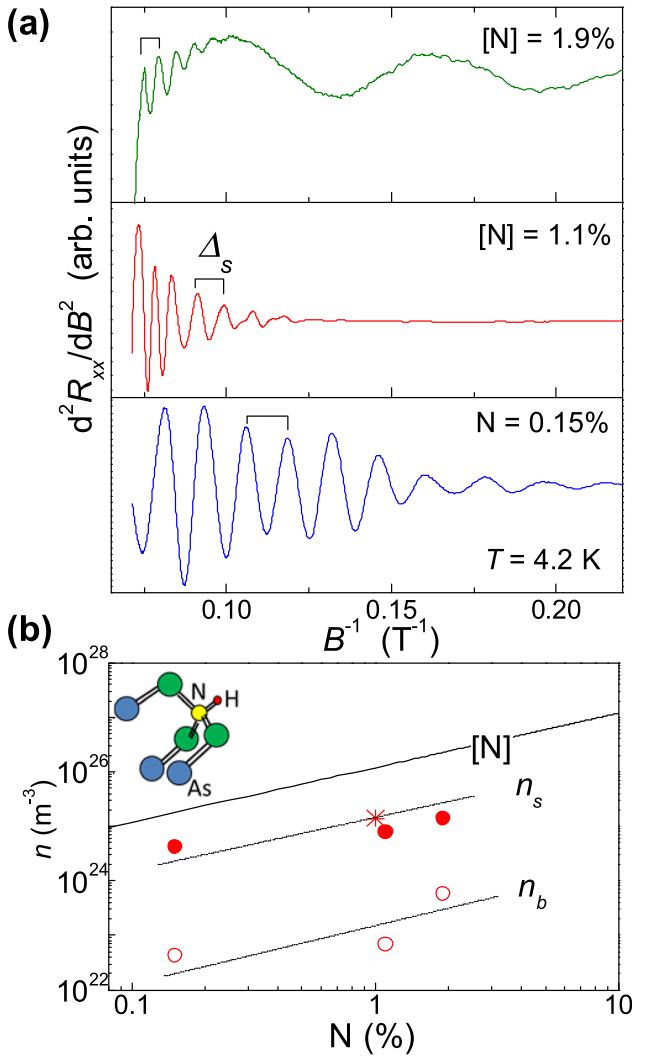

FIG. 2. (a) d^2R_{xx}/d^2B versus $1/B$ for hydrogenated In(AsN) epilayers with [N] = 0.15, 1.1, and 1.9% ($B > 5$ T and $T = 4.2$ K). The period Δ_S of the short-period SdH oscillations is indicated for each sample. (b) Dependence of the electron density on [N] in hydrogenated In(AsN) as derived from the period of the SdH oscillations ($T = 4.2$ K). Circles and dots are for In(AsN) epilayers hydrogenated under the same conditions ($D_H = 10^{20}$ ions/m^2, $t_H = 9$ min, $T_H = 300$ °C). The star corresponds to an In(AsN) epilayer hydrogenated with higher doses ($D_H = 4 \times 10^{21}$ and 10^{23} ions/m^2 for $t_H = 1$ and 6 h, respectively), as reported in Ref. 7. The continuous line shows the density of N-atoms. Dotted lines are guides to the eye. The inset is a sketch of an H-bond-center site next to nitrogen, H(BC$_N$), as described in Ref. 8.

The H-induced increase in the electron density tends to saturate to about 10% of the total N-concentration with H-doses increasing from $D_H = 10^{20}$ to $10^{23}\,\text{m}^{-2}$, see Figure 2(b). Correspondingly, the Fermi energy E_F remains pinned to a value in the range 0.2 to 0.4 eV above the conduction band minimum of In(AsN).[14]

Given the observation of SdH oscillations with two distinct electrons densities, we use a conduction model with two parallel channels[15] to determine the width of each channel and its contribution to the overall Hall resistance, R_{xy}, given by

$$R_{xy}(B) = \frac{\left[\mu_b\sigma_b d_b + \mu_s\sigma_s d_s + \mu_b\mu_s(\mu_s\sigma_b d_b + \mu_b\sigma_s d_s)B^2\right]B}{(\sigma_b d_b + \sigma_s d_s)^2 + (\mu_s\sigma_b d_b + \mu_b\sigma_s d_s)^2 B^2}, \quad (1)$$

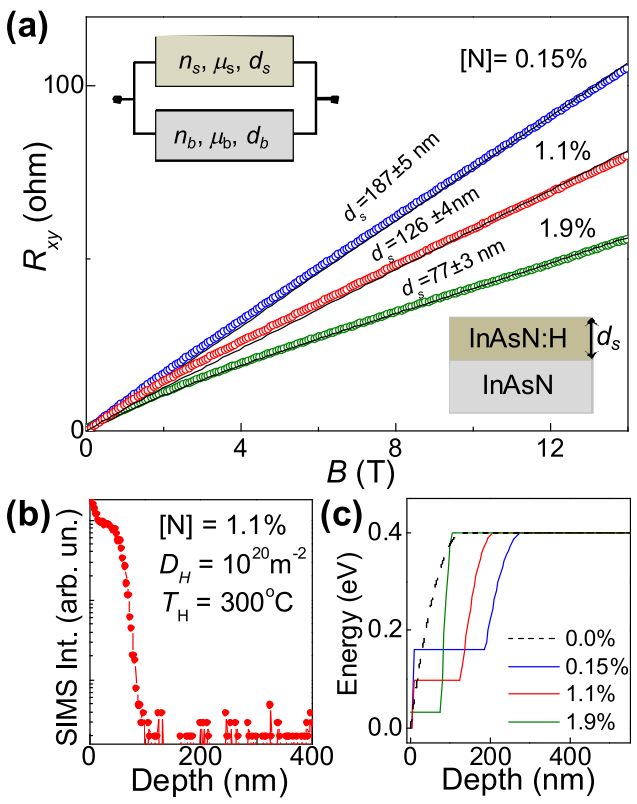

FIG. 3. (a) Measured (dots) and calculated (black lines) Hall resistance, R_{xy}, versus B for In(AsN) epilayers hydrogenated under the same conditions ($D_H = 10^{20}$ ions/m^2, $t_H = 9$ min, $T_H = 300\,^\circ$C). (b) ^{2}H SIMS profile for [N] = 1.1% ($D_H = 10^{20}$ ions/m^2, $t_H = 9$ min, $T_H = 300\,^\circ$C). (c) Bending of the conduction band for InAs (dashed line) and In(AsN) (continuous lines) as derived from the Poisson's equation. Here, we have used: (i) the measured electron densities; (ii) the thickness d_s of the H-containing layer; and (iii) a surface Fermi level pinned at a value of 0.4 eV above the conduction band minimum.[16]

where d_s is the thickness of the surface channel, $d_b = d - d_s$, d is the thickness of the epilayer, and $\sigma_{s(b)}$ and $\mu_{s(b)}$ are the electron conductivity and mobility of the surface (s) and bulk (b) layers, respectively. Figure 3(a) shows least-square fitting of Eq. (1) to the Hall resistance curves, $R_{xy}(B)$, for [N] = 0.15, 1.1, and 1.9%, each reproducing accurately the non-linear B-dependence of R_{xy}. Each fit uses only one fitting parameter, d_s, with all other parameters fixed to the values measured experimentally: The carrier densities, n_s and n_b, of the two channels are derived from the measured period of the SdH oscillations; the mobilities, μ_s and μ_b, are obtained from the condition $\mu B > 1$ required to observe each set of oscillations; and the epilayer thickness d is set to the nominal value of 1 μm (see Table I). The same set of parameters was used to fit the values of the transverse resistance at $B = 0$ T, i.e., $R_{xx}(0) = LW^{-1}(\sigma_s d_s + \sigma_b d_b)^{-1}$, where $L = 750\,\mu$m and $W = 250\,\mu$m.

Our data analyses indicate that d_s decreases from 187 to 77 nm with increasing [N] from 0.15 to 1.9%, from which we infer a smaller penetration depth of H at higher [N] and an almost constant electron sheet density ($n_s d_s \approx 10^{18}$ m^{-2}). As shown in Figure 3(b), the SIMS profile for ^{2}H has a box-shaped form from which we estimate a ^{2}H penetration depth of ~100 nm for [N] = 1.1%. This is close to the value of $d_s = 128$ nm inferred from the magneto-transport data. Thus, we propose that under the small H-doses and relatively low hydrogenation temperatures used in this work, H-atoms tend to be effectively trapped by the N-atoms in a thin (≈100 nm) subsurface layer. In this region, the H-atoms can strongly bind to nitrogen and form H-N donor complexes H(BC$_N$), in which H occupies the bond-center site between a N- and an In-atom (see inset of Figure 2(b)).[8]

We estimate the resistance, R_S, of the surface channel to be $R_S = (en_s\mu_s)^{-1}L/(d_s W) = 46$, 97, and 158 Ω for [N] = 0.15, 1.1, and 1.9%, respectively. These values are comparable to the total measured resistance ($R = 42$, 82, 58 Ω) and can be significantly smaller than the resistance of the bulk layer, i.e., $R_b = (en_b\mu_b)^{-1}L/(d_b W) = 440$, 546, and 90 Ω. The smaller value of R_b for [N] = 1.9% is due the larger bulk electron density, n_b (see Figure 2(b)). Thus, the contribution of the H-containing subsurface layer to the conductivity is significant and can be dominant even in thick (~1 μm) epilayers. This is in stark contrast to the behavior of N-free InAs. From the analysis of the Hall resistance using the two channels model, we find that the H-induced increase of the electron density is negligible and that the surface accumulation layer has an electron sheet density of ~10^{16} m^{-2}, significantly smaller than for In(AsN). Furthermore, whereas in InAs the charge is located on the surface thus leading to a bending of the bands and the formation of two-dimensional (2D) accumulation layer,[16] in In(AsN), the spatially uniform density of donors across the thin (~100 nm) subsurface region of the epilayer and large electron sheet density lead to a 3D electron gas near the surface (Figure 3(c)).

We note that despite the incorporation of H and the relatively large electron sheet density (≈10^{18} m^{-2}), the In(AsN) surface channel has a relatively high mobility (>0.1 m^{2}V^{-1}s^{-1}) at both low and room temperature; also, the H-containing In(AsN) layer retains a high electron sheet density after many thermal cycles from $T = 4$ K to 300 K, and thermal annealing in argon at temperatures up to 473 K, thus indicating a stable modification of the In(AsN) alloy by hydrogen, an essential requirement for future applications of this compound.

TABLE I. Parameters of the surface (s) and bulk (b) conductivity channels for hydrogenated In(AsN) epilayers ($D_H = 10^{20}$ ions/m^2, $t_H = 9$ min, $T_H = 300\,^\circ$C). These were derived from the period of the Shubnikov de Haas oscillations (n_s, n_b, μ_s, μ_b) and from the analysis of the Hall resistance (R_{xy}) and transverse magneto-resistance (R_{xx}) by a model with two parallel conducting channels, the shallower of which has width d_s.

N (%)	n_s (m^{-3})	n_b (m^{-3})	μ_s (m^{2}V^{-1}s^{-1})	μ_b (m^{2}V^{-1}s^{-1})	d_s (nm)
0.15	$(4.2 \pm 0.5) \times 10^{24}$	$(4.3 \pm 0.5) \times 10^{22}$	0.52 ± 0.07	1.22 ± 0.26	187 ± 5
1.1	$(8.1 \pm 1.4) \times 10^{24}$	$(6.9 \pm 0.7) \times 10^{22}$	0.19 ± 0.03	0.57 ± 0.02	126 ± 4
1.9	$(1.4 \pm 0.1) \times 10^{25}$	$(5.9 \pm 0.4) \times 10^{23}$	0.11 ± 0.01	0.38 ± 0.07	77 ± 3

In summary, we have shown that the *n*-type surface conductivity of In(AsN) is modified by the controlled incorporation of H-atoms through the formation of donors within a well-defined subsurface region of the In(AsN) epilayer. For a fixed H-dose, the width of this channel decreases with the increase in concentration of N-atoms, which act as effective barriers to the H-diffusion thus producing box-shaped ^{2}H-diffusion profiles and a high electron sheet density ($\sim 10^{18}\,m^{-2}$). Our findings will stimulate theoretical studies of H-diffusion and energy levels in mid-infrared III-N-Vs, where hydrogen, being either an unintentional or intentional dopant, affects surface electronic properties.[11] Furthermore, our results open up perspectives for employing mid-infrared In(AsN) in applications that exploit its *n*-type surface conductivity, ranging from gas sensing[12] to "all semiconductors" plasmonic waveguides[13] for mid-infrared photonics. In particular, the controlled photodissociation of H-N donor complexes by a focused laser beam[4] or the selective H-incorporation by masking may provide a route for writing conducting paths and printed circuits on a single substrate.

This work was supported by EPSRC.

[1]W. Shan, W. Walukiewicz, J. W. Ager III, E. E. Haller, J. F. Geisz, D. J. Friedman, J. M. Olson, and S. R. Kurtz, Phys. Rev. Lett. **82**, 1221 (1999).
[2]E. P. O'Reilly, A. Lindsay, P. J. Klar, A. Polimeni, and M. Capizzi, Semicond. Sci. Technol. **24**, 033001 (2009).
[3]S. Birindelli, M. Felici, J. Wildmann, A. Polimeni, M. Capizzi, A. Gerardino, S. Rubini, F. Martelli, A. Rastelli, and R. Trotta, Nano Lett. **14**, 1275 (2014).
[4]N. Balakrishnan, G. Pettinari, O. Makarovsky, M. Hopkinson, and A. Patanè, Appl. Phys. Lett. **104**, 242110 (2014).
[5]L. Wen, F. Bekisli, M. Stavola, W. B. Fowler, R. Trotta, A. Polimeni, M. Capizzi, S. Rubini, and F. Martelli, Phys. Rev. B **81**, 233201 (2010).
[6]Y. Y. Ke, M. H. Ya, Y. F. Chen, J. S. Wang, and H. H. Lin, Appl. Phys. Lett. **80**, 3539 (2002).
[7]N. V. Kozlova, G. Pettinari, O. Makarovsky, N. Mori, A. Polimeni, M. Capizzi, Q. D. Zhuang, A. Krier, and A. Patanè, Phys. Rev. B **87**, 165207 (2013).
[8]A. Janotti, S. B. Zhang, S.-H. Wei, and C. G. Van deWalle, Phys. Rev. Lett. **89**, 086403 (2002).
[9]A. Krier, *Mid-infrared Semiconductor Optoelectronics*, Springer Series in Optical Sciences Vol. 118 (Springer, 2006).
[10]W. Walukiewicz, Phys. Rev. B **37**, 4760 (1988).
[11]C. W. M. Castleton, A. Höglund, M. Göthelid, M. C. Qian, and S. Mirbt, Phys. Rev. B **88**, 045319 (2013).
[12]A. Dedigama, M. Angelo, P. Torrione, T.-H. Kim, S. Wolter, W. Lampert, A. Atewologun, M. Edirisoorya, L. Collins, T. F. Kuech, M. Losurdo, G. Bruno, and A. Brown, J. Phys. Chem. C **116**, 826 (2012).
[13]D. Li and C. Z. Ning, Opt. Express **19**, 14594 (2011).
[14]The electron energy dispersion of InAs is modelled as $\varepsilon(\boldsymbol{k})[1+\alpha\varepsilon(\boldsymbol{k})] = \hbar^2k^2/2m_0^*$, where $\alpha = 1/E_g$ eV^{-1}, $E_g = 0.42$ eV is the band gap energy at 4.2K, $m_0^* = 0.025\ m_e$ is the electron effective mass at $\boldsymbol{k}=0$, and m_e is the electron mass in vacuum. In In(AsN), the energy dispersion is modified by the interaction of the N-level with the conduction band states, described here by a two-level band-anticrossing model with an interaction parameter $V_N = 2.5$ eV and a N-level at 1.0 eV above the conduction band minimum of InAs.
[15]A. Nedoluha and K. M. Koch, Z. Phys. **132**, 608 (1952).
[16]P. D. C. King, T. D. Veal, C. F. McConville, J. Zúñiga-Pérez, V. Muñoz-Sanjosé, M. Hopkinson, E. D. L. Rienks, M. F. Jensen, and Ph. Hofmann, Phys. Rev. Lett. **104**, 256803 (2010).